Biodistribution and Radiation Dosimetry of the Serotonin Transporter Ligand ^{11}C-DASB Determined from Human Whole-Body PET

Jian-Qiang Lu, MD, PhD; Masanori Ichise, MD; Jeih-San Liow, PhD; Subroto Ghose, MD, PhD; Doug Vines, BSc; and Robert B. Innis, MD, PhD

Molecular Imaging Branch, National Institute of Mental Health, National Institutes of Health, Bethesda, Maryland

^{11}C-Labeled 3-amino-4-(2-dimethylaminomethylphenylsulfanyl)-benzonitrile (DASB) is a selective radioligand for the in vivo quantitation of serotonin transporters (SERTs) using PET. The goal of this study was to provide dosimetry estimates for ^{11}C-DASB based on human whole-body PET. **Methods:** Dynamic whole-body PET scans were acquired for 7 subjects after the injection of 669 ± 97 MBq (18.1 ± 2.6 mCi) of ^{11}C-DASB. The acquisition for each subject was obtained at 14 time points for a total of 115 min after injection of the radioligand. Regions of interest were placed over compressed planar images of source organs that could be visually identified to generate time–activity curves. Radiation burden to the body was calculated from residence times of these source organs using the MIRDOSE3.1 program. **Results:** The organs with high radiation burden included the lungs, urinary bladder wall, kidneys, gallbladder wall, heart wall, spleen, and liver. The activity peaked within 10 min after the injection of ^{11}C-DASB for all these organs except two—the excretory organs gallbladder and urinary bladder wall, which had peak activities at 32 and 22 min, respectively. Monoexponential fitting of activity overlying the urinary bladder suggested that approximately 12% of activity was excreted via the urine. Simulations in which the urinary voiding interval was decreased from 4.8 to 0.6 h produced only modest effects on the dose to the urinary bladder wall. With a 2.4-h voiding interval, the calculated effective dose was 6.98 μGy/MBq (25.8 mrem/mCi). **Conclusion:** The estimated radiation burden of ^{11}C-DASB is relatively modest and would allow multiple PET examinations of the same research subject per year.

Key Words: ^{11}C-DASB; serotonin transporter; dosimetry; whole-body biodistribution; PET

J Nucl Med 2004; 45:1555–1559

The neurotransmitter serotonin (5-HT) plays an important role in the regulation of many brain functions, including mood, appetite, sleep, pain, and aggressive behavior (*1*). The concentration of synaptic 5-HT is directly controlled by its reuptake into the presynaptic terminals via the serotonin transporter (SERT). Alterations in SERT densities have been noted in a large number of neuropsychiatric conditions, including depression, anxiety disorders, schizophrenia, drug abuse, alcoholism, eating disorders, Alzheimer's disease, and Parkinson's disease (*2–4*). SERT is also the molecular target of many antidepressant medications (*5–7*) and psychostimulants with abuse potential, such as cocaine and amphetamine (*7,8*). Therefore, in vivo imaging of the regional brain distribution of SERT is an important tool for studying the role of the 5-HT system in the pathophysiology and treatment of neuropsychiatric disorders.

Several PET radioligands for SERT are available to measure regional SERT levels in the brain (*9*). The radioligand 3-amino-4-(2-dimethylaminomethyl-phenylsulfanyl)-benzonitrile (DASB), labeled with ^{11}C in the *N*-methyl position, is arguably the best for PET of SERT in the human brain (*9–13*). ^{11}C-DASB has high affinity and selectivity, displaying moderately high specific-to-nonspecific ratios in vivo (*10–12*), and ^{11}C-DASB PET data allow accurate quantification of SERT binding parameters (*12,13*). Radiation dosimetry estimates based on whole-body distribution of activity in rats (*14*) and monkeys (*15*) were recently reported for ^{11}C-DASB. Because of likely species differences (*15,16*), the present study was performed with whole-body PET on healthy human subjects to measure organ activities and estimate the associated radiation-absorbed doses.

MATERIALS AND METHODS

Radiopharmaceutical Preparation

The radiotracer ^{11}C-DASB was synthesized as previously described (*14*) by ^{11}C-methyliodide reaction with the corresponding desmethyl precursor. The radiochemical purities of syntheses used for this study were 94.4% ± 1.5%, with corresponding specific activities of 50.5 ± 11.9 GBq/μmol (1.37 ± 0.32 Ci/μmol) at the time of injection. These and subsequent data are expressed as mean ± SD.

Subjects

The study was approved by the Radiation Safety Committee of the National Institutes of Health and the Institutional Review

Received Nov. 17, 2003; revision accepted Mar. 12, 2004.

For correspondence or reprints contact: Jian-Qiang Lu, MD, PhD, Molecular Imaging Branch, NIMH, National Institutes of Health, Bldg. 1, Room B3-10, 1 Center Dr., MSC 0135, Bethesda, MD 20892-0135.

E-mail: lujq@intra.nimh.nih.gov

Board of the National Institute of Mental Health. Two male and 5 female healthy volunteers (age, 35 ± 11 y [range, 22–50 y]; weight, 72 ± 12 kg) participated in the study after providing written informed consent. All subjects were free of medical or neuropsychiatric illness on the basis of a screening assessment comprising history, physical examination, routine blood and urine tests, and electrocardiography. Within 3 mo before and approximately 24 h after tracer administration, every subject underwent standard laboratory tests including complete blood count; serum chemistries; thyroid, liver, and kidney function tests; and urinalysis.

PET Data Acquisition

One preinjection transmission scan and serial dynamic emission scans were obtained with an Advance tomograph (General Electric Medical Systems). The scanner was cross-calibrated weekly to a well counter with a known activity of ^{18}F in a 16-cm-diameter cylindric phantom. In addition, the camera was checked daily for constancy with a ^{137}Cs source. Imaging of each subject comprised 7 consecutive sections of the body from head to mid thigh. Each subject was positioned with head fixation devices and elastic body-restraining bandages to minimize head and body movement during each scan. Electrocardiography findings, blood pressure, and heart and respiration rates were monitored for all subjects during scanning.

Before injection of the radioligand, a 21-min whole-body transmission scan was obtained using ^{68}Ge rods for subsequent attenuation correction of the corresponding emission images. The dynamic emission scan of 14 frames was acquired after intravenous administration of 669 ± 97 MBq (18.1 ± 2.6 mCi) of ^{11}C-DASB. The acquisition of each frame comprised the following: starting an emission scan at the first bed position, for the head; moving the bed caudally to the next section; scanning 7 sections consecutively for the same period, with the bed moved at six 3-s intervals; and taking 13 s to reposition the bed back to the first section after completing that frame. Acquisition of 14 frames (4 × 0.25, 3 × 0.5, 3 × 1, 3 × 2, and 1 × 4 min, × 7 sections, plus intervals for moving the bed between sections) approximated 115 min, except for one subject whose scan was terminated 30 min earlier (2 frames short) because of a need to urinate.

Horizontal tomographic images were compressed in the anteroposterior dimension into a single planar image. The compressed planar images were analyzed with pixelwise modeling software (PMOD, version 2.4; PMOD Group). Our previous study (*15*) indicated that analysis of such compressed planar images is comparable to that of tomographic images, but with a slight overestimation (i.e., conservative calculation) of organ radiation burden. Regions of interest were drawn in source organs that could be identified: brain, lungs, heart, liver, gallbladder, spleen, kidneys, and urinary bladder. Generous regions of interest were placed to ensure that all accumulated radioactivity in each organ was encompassed. Activity in the remainder of the body was calculated at each time point by subtracting that present in the identified source organs from the decayed value of the injected activity.

Residence Time Calculation

Activity in the source organs (non–decay corrected) was expressed as a percentage of the injected dose (%ID) and plotted against time. The area under the time–activity curve (%ID versus time) for each organ from time zero to infinity is equal to residence time (in hours). The area under the curve was calculated with the trapezoid rule, with the assumptions that there was no activity at time 0 and that after the last time point, activity decreased only by physical decay (i.e., no biologic clearance after the last time point).

Because each whole-body scan consisted of 7 consecutive sections from head to mid thigh, measurements of activities in lower organs (such as the urinary bladder) were later than those for the head, with an interval varying from seconds to minutes depending on the particular section and frame. Thus, we standardized the time points of different sections to the time point of the first section (i.e., that overlying the head) using liner interpolation between the current and adjacent frames. The reason for this standardization was to estimate the remainder-of-body activity, which was calculated as the injected activity decayed to the common time point minus the sum of all source organ activities at that same time point.

Organ-Absorbed Dose

Because no urination was allowed during scanning, the activity overlying the bladder represented the total urinary excretion. The mean cumulative urine activity curve of 7 subjects was fitted with a monoexponential curve, and the total excretion in urine in terms of fraction of the injected dose and biologic half-life was determined. The dynamic bladder model (*17*), implemented in MIRDOSE3.1 (Oak Ridge Institute for Science and Education), was applied to calculate residence time with several voiding intervals: 0.6, 1.2, 2.4, and 4.8 h. Organ-absorbed doses were based on the MIRD scheme (*18*) of a 70-kg adult, using the residence times calculated above.

RESULTS

Electrocardiography findings, blood pressure, heart rate, and respiration rate showed no apparent change after administration of ^{11}C-DASB. In addition, no effects were noted in any of the blood and urine tests acquired approximately 24 h after administration of this radioligand.

Brain, lungs, heart, liver, gallbladder, spleen, kidneys, and urinary bladder were visually identified as organs with moderate to high activities (Fig. 1). Uptake of ^{11}C-DASB in the lungs was strikingly high, with a peak of 53.1 %ID, always measured in the first whole-body scan and typically from 18 to 46 s after injection. Peak uptake in the heart, liver, brain, kidneys, and spleen was 5.3%, 4.3%, 4.0%, 1.4%, and 0.8 %ID, respectively, and all occurred within 10 min. The maximal uptake in the gallbladder was 0.3 %ID,

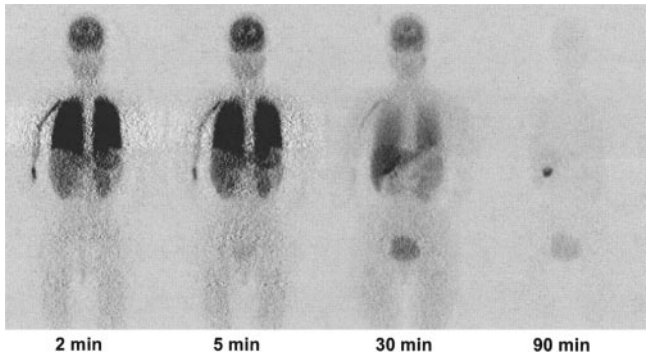

FIGURE 1. Compressed whole-body planar emission images demonstrating biodistribution of radioactivity in a healthy subject 2, 5, 30, and 90 min after intravenous injection of ^{11}C-DASB.

occurring at 32 min. Figure 2 displays time–activity curves for these organs at the average time points at which they were imaged.

The mean accumulation of activity over the urinary bladder for all subjects is shown in Figure 3, with a monoexponential curve fit. With a mean r^2 value of 0.997, this curve well described the accumulated activity over the bladder. According to this fit, the biologic half-life was 51 min. The asymptote of the curve implies that 12 %ID was excreted in urine. The dynamic bladder model estimated residence times of 0.0083, 0.0013, 0.0158, and 0.0162 h for bladder contents at respective urine-voiding intervals of 0.6, 1.2, 2.4, and 4.8 h.

Table 1 summarizes residence times calculated from whole-body images of 7 subjects. From these mean residence times and the percentage of activity excreted via the urine, radiation-absorbed dose estimates were calculated for urine-voiding intervals of 0.6, 1.2, 2.4, and 4.8 h. The changes in urine-voiding intervals caused only modest effects on the dose to the urinary bladder wall. The effective doses were 6.68, 6.87, 6.98, and 7.00 μSv/MBq at respective urine-voiding intervals of 0.6, 1.2, 2.4, and 4.8 h. With a 2.4-h interval (Table 2), the highest absorbed organ doses (μGy/MBq) were to the lungs (32.8), urinary bladder wall (12.0), kidneys (9.28), and gallbladder wall (9.27).

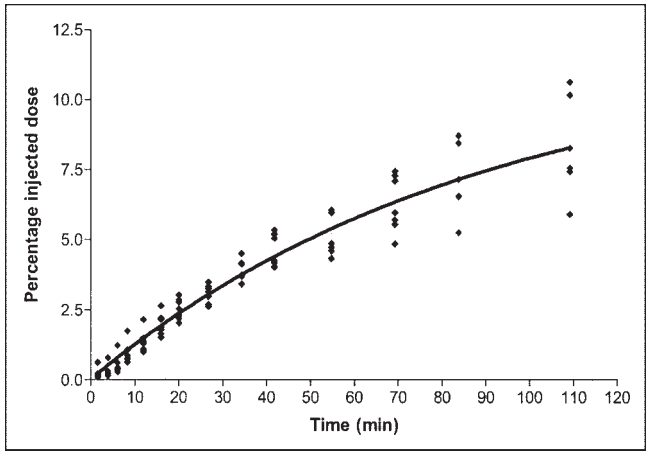

FIGURE 3. Cumulative urinary excretion of decay-corrected radioactivity after intravenous administration of ^{11}C-DASB to 7 healthy subjects. Data points reflect actual radioactivity measured for bladder by PET. Solid line is monoexponential fitting with Prism software (version 3.0; GraphPad Software Inc.) for the averages of 7 subjects. The fraction excreted via urine reached a maximal (asymptotic) value of approximately 12%, with a half-life of 51 min.

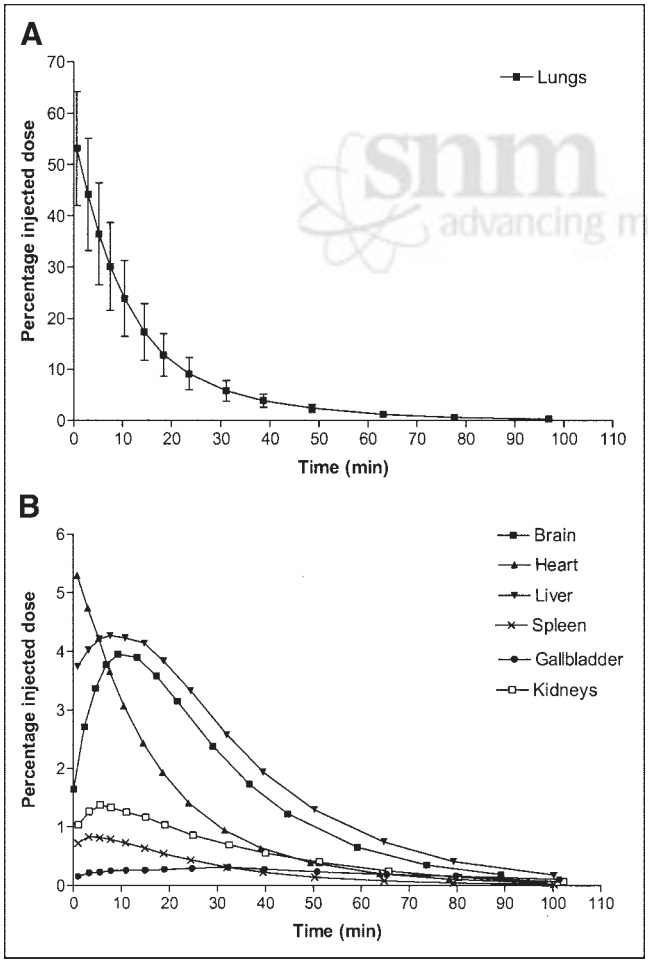

FIGURE 2. Time–activity curves for ^{11}C-DASB determined from serial PET of organs. (A) Graph showing data expressed as mean ± SD for 7 subjects and not corrected for radioactive decay. (B) Graph showing data expressed as averages for 7 subjects and not corrected for radioactive decay.

DISCUSSION

The present study estimated the dosimetry of ^{11}C-DASB based on whole-body PET in human subjects. With the calculated effective dose (7 μSv/MBq, or 26 mrem/mCi), the injected activities of 523–788 MBq (14–22 mCi) that are commonly used for human brain imaging would yield an effective dose of 3.7–5.5 mSv (364–572 mrem). According to the intramural guidelines of the National Institutes of Health, adult research subjects should receive no more than a 0.05-Sv (5 rem) effective dose per year (*19*). Based on

TABLE 1
Residence Times Calculated from Whole-Body Images of 7 Subjects

Organ	Residence time (h)
Brain	0.024 ± 0.005
Gallbladder	0.003 ± 0.002
Heart	0.017 ± 0.006
Kidneys	0.009 ± 0.004
Liver	0.030 ± 0.007
Lungs	0.126 ± 0.035
Spleen	0.004 ± 0.001
Remainder of body	0.252 ± 0.033

Values are means ± SDs for the 7 subjects.

TABLE 2
Radiation Dose Estimates for ^{11}C-DASB

Target organ	mGy/MBq	rad/mCi
Adrenals	3.16E-03	1.17E-02
Brain	5.77E-03	2.14E-02
Breasts	2.36E-03	8.73E-03
Gallbladder wall	9.27E-03	3.43E-02
Lower large intestine wall	2.11E-03	7.82E-03
Small intestine	2.18E-03	8.08E-03
Stomach	2.46E-03	9.09E-03
Upper large intestine wall	2.21E-03	8.19E-03
Heart wall	8.21E-03	3.04E-02
Kidneys	9.28E-03	3.43E-02
Liver	6.41E-03	2.37E-02
Lungs	3.28E-02	1.21E-01
Muscle	2.09E-03	7.72E-03
Ovaries	2.18E-03	8.06E-03
Pancreas	3.03E-03	1.12E-02
Red marrow	2.33E-03	8.63E-03
Bone surfaces	2.25E-03	8.34E-03
Skin	1.60E-03	5.91E-03
Spleen	7.40E-03	2.74E-02
Testes	1.74E-03	6.44E-03
Thymus	2.98E-03	1.10E-02
Thyroid	2.06E-03	7.63E-03
Urinary bladder wall	1.20E-02	4.43E-02
Uterus	2.45E-03	9.05E-03
Total body	2.75E-03	1.02E-02
	mSv/MBq	rem/mCi
Effective dose equivalent	8.01E-03	2.96E-02
Effective dose	6.98E-03	2.58E-02

Urine-voiding interval is 2.4 h.

these results, this 0.05-Sv (5 rem) limit corresponds to ~7,104 MBq (~192 mCi) of ^{11}C-DASB per subject per year. In other words, this limit allows as many as 12 injections of 555 MBq (15 mCi) to a subject within a year.

In the present study, the injected mass doses of DASB (~29.5 nmol) produced no change in vital signs or in the results of electrocardiography and standard laboratory tests. Therefore, ^{11}C-DASB appears to be safe from both pharmacologic and radiation perspectives.

The present study used a PET protocol similar to that for our monkey study (*15*) but with a few improvements: increasing the number of subjects studied, identifying the heart as an additional source organ, and separating gallbladder from liver because of its cumulated activity and excretion of this radionuclide (*14–16*). The value of the effective dose presented here (7.0 μSv/MBq) is slightly higher than the values reported for monkeys (6.4 μSv/MBq) and rats (5.5 μSv/MBq) (*14,15*). This discrepancy may be attributable to species differences in the pharmacokinetics of ^{11}C-DASB (*15,16*). Obviously, the major contributor to the difference in biodistribution of this radioligand was lung uptake, which reached a maximum of 53.1 %ID immediately after injection in humans but only 24 %ID at approximately 1.5 min in monkeys (*15*) and only 6 %ID in rats (*14*). High uptake in human lungs has been reported for the other SERT radioligands, such as ^{11}C-labeled (+)-6β-(4-methylthiophenyl)-1,2,3,5,6α, 10β-hexahydropyrrolo (2,1-a)isoquinoline and ^{11}C-labeled cyanoimipramine (*20*), as well as monoamine transporter radioligand ^{123}I-labeled methyl 3β-(4-iodophenyl)tropane-2β-carboxylate (*21*), but not in rodent lungs for ^{11}C-labeled dapoxetine-HCl (*22*). The potential mechanisms underlying such a high uptake of SERT radioligands in human lungs include specific binding on pulmonary membranes for the uptake of circulating 5-HT, nonspecific binding, and a large blood volume (*23–25*). Nevertheless, washout of ^{11}C-DASB from human lungs was fast and decreased by more than 50% within 10 min, thereby reducing the radiation burden to this organ.

In contrast to the lungs, other organs had a relatively lower radiation burden. The second-highest organ dose was to the urinary bladder wall (12.0 μGy/MBq, or 44.3 mrad/mCi, with a voiding interval of 2.4 h). This dose from the human study is relatively lower than doses derived from monkey (25.0 μGy/MBq) and rat (32.2 μGy/MBq) studies (*14,15*). We could not visualize the ^{11}C-DASB activity in the gastrointestinal tract within the time frame of imaging acquisition. Because only a small proportion (up to 12%) of activity is excreted via the urinary tract, and activity was clearly seen in the liver and gallbladder, one would presume that most activity was excreted via the gastrointestinal tract but after substantial physical decay.

CONCLUSION

^{11}C-DASB exhibited a favorable profile of radiation burden that would allow multiple PET studies of the same subject. The radiation safety of ^{11}C-DASB and its imaging merits make it a superior radioligand for studying neuropsychiatric disorders.

ACKNOWLEDGMENTS

We gratefully acknowledge Michael Channing and William Eckelman for the radiosynthesis of ^{11}C-DASB and Lisa Coronado for critical review of the "Materials and Methods" and "Results" sections.

REFERENCES

1. Lucki I. The spectrum of behaviors influenced by serotonin. *Biol Psychiatry.* 1998;44:151–162.
2. Chen CP, Alder JT, Bowen DM, et al. Presynaptic serotonergic markers in community-acquired cases of Alzheimer's disease: correlations with depression and neuroleptic medication. *J Neurochem.* 1996;66:1592–1598.
3. Abi-Dargham A, Laruelle M, Aghajanian GK, Charney D, Krystal J. The role of serotonin in the pathophysiology and treatment of schizophrenia. *J Neuropsychiatry Clin Neurosci.* 1997;9:1–17.
4. Deakin JF. The role of serotonin in panic, anxiety and depression. *Int Clin Psychopharmacol.* 1998;13(suppl 4):S1–S5.
5. Charney DS. Monamine dysfunction and the pathophysiology and treatment of depression. *J Clin Psychiatry.* 1998;59:11–14.
6. Kugaya A, Seneca NM, Snyder PJ, et al. Changes in human in vivo serotonin and dopamine transporter availabilities during chronic antidepressant administration. *Neuropsychopharmacology.* 2003;28:413–420.

7. Iversen L. Neurotransmitter transporters: fruitful targets for CNS drug discovery. *Mol Psychiatry.* 2000;5:357–362.
8. Ramamoorthy S, Blakely RD. Phosphorylation and sequestration of serotonin transporters differentially modulated by psychostimulants. *Science.* 1999;285: 763–766.
9. Huang Y, Hwang DR, Narendran R, et al. Comparative evaluation in nonhuman primates of five PET radiotracers for imaging the serotonin transporters: [^{11}C]McN5652, [^{11}C]ADAM, [^{11}C]DASB, [^{11}C]DAPA, and [^{11}C]AFM. *J Cereb Blood Flow Metab.* 2002;22:1377–1298.
10. Wilson AA, Ginovart N, Schmidt M, Meyer JH, Threlkeld PG, Houle S. Novel radiotracers for imaging the serotonin transporter by positron emission tomography: synthesis, radiosynthesis, and *in vitro* and *ex vivo* evaluation of ^{11}C-labeled 2-(phenylthio)araalkylamines. *J Med Chem.* 2000;43:3103–3110.
11. Houle S, Ginovart N, Hussey D, Meyer JH, Wilson AA. Imaging the serotonin transporter with positron emission tomography: initial human studies with [^{11}C]DAPP and [^{11}C]DASB. *Eur J Nucl Med.* 2000;27:1719–1722.
12. Ginovart N, Wilson AA, Meyer JH, Hussey D, Houle S. Positron emission tomography quantification of [^{11}C]DASB binding to the human serotonin transporter: modeling strategies. *J Cereb Blood Flow Metab.* 2001;21:1342–1253.
13. Ichise M, Liow JS, Lu JQ, et al. Linearized reference tissue parametric imaging methods: application to [^{11}C]DASB PET studies of the serotonin transporter in human brain. *J Cereb Blood Flow Metab.* 2003;23:1096–1112.
14. Wilson AA, Ginovart N, Hussey D, Meyer J, Houle S. In vitro and in vivo characterisation of [^{11}C]-DASB: a probe for in vivo measurements of the serotonin transporter by positron emission tomography. *Nucl Med Biol.* 2002;29: 509–515.
15. Tipre DN, Lu JQ, Fujita M, Ichise M, Vines D, Innis RB. Radiation dosimetry estimates for the PET serotonin transporter probe [^{11}C]DASB determined from whole-body imaging in nonhuman primates. *Nucl Med Commun.* 2004;25:81–86.
16. Wrobel MC, Carey JE, Sherman PS, Kilbourn MR. Simplifying the dosimetry of carbon-11-labeled radiopharmaceuticals. *J Nucl Med.* 1997;38:654–660.
17. Cloutier RJ, Smith SA, Watson EE, Snyder WS, Warner GG. Dose to the fetus from radionuclides in the bladder. *Health Phys.* 1973;25:147–161.
18. Loevinger R, Budinger TF, Watson EE. *MIRD Primer for Absorbed Dose Calculations.* New York. NY: Society of Nuclear Medicine; 1991.
19. Radiological protection and safety in medicine. *Ann ICRP.* 1996;26. ICRP publication 73.
20. Takano A, Suhara T, Sudo Y, et al. Comparative evaluation of two serotonin transporter ligands in the human brain: [^{11}C](+)McN5652 and [^{11}C]cyano-imipramine. *Eur J Nucl Med.* 2002;29:1289–1297.
21. Seibyl JP, Wallace E, Smith EO, et al. Whole-body biodistribution, radiation absorbed dose and brain SPECT imaging with iodine-123-CIT in healthy human subjects. *J Nucl Med.* 1994;35:764–770.
22. Livni E, Satterlee W, Robey RL, et al. Synthesis of [^{11}C]dapoxetine.HCI, a serotonin re-uptake inhibitor: biodistribution in rat and preliminary PET imaging in the monkey. *Nucl Med Biol.* 1994;21:669–675.
23. Hart CM, Block ER. Lung serotonin metabolism. *Clin Chest Med.* 1989;10:59–70.
24. Ramamoorthy S, Bauman AL, Moore KR, et al. Antidepressant- and cocaine-sensitive human serotonin transporter: molecular cloning, expression, and chromosomal localization. *Proc Natl Acad Sci USA.* 1993;90:2542–2546.
25. Paczkowski NJ, Vuocolo HE, Bryan-Lluka LJ. Conclusive evidence for distinct transporters for 5-hydroxytryptamine and noradrenaline in pulmonary endothelial cells of the rat. *Naunyn Schmiedebergs Arch Pharmacol.* 1996;353:423–430.

JNM The Journal of NUCLEAR MEDICINE

Biodistribution and Radiation Dosimetry of the Serotonin Transporter Ligand ^{11}C-DASB Determined from Human Whole-Body PET

Jian-Qiang Lu, Masanori Ichise, Jeih-San Liow, Subroto Ghose, Doug Vines and Robert B. Innis

J Nucl Med. 2004;45:1555-1559.

The Journal of Nuclear Medicine is published monthly.
SNMMI | Society of Nuclear Medicine and Molecular Imaging
1850 Samuel Morse Drive, Reston, VA 20190.
(Print ISSN: 0161-5505, Online ISSN: 2159-662X)

SNMMI SOCIETY OF NUCLEAR MEDICINE AND MOLECULAR IMAGING